International Research Journal of Engineering and Technology (IRJET) e-ISSN: 2395-0056
Volume: 08 Issue: 06 | June 2021 www.irjet.net p-ISSN: 2395-0072

Wind Effect on a Parabolic Trough Concentrator for Medium Size

Mohmad H. Ahmed[1]

[1]*Solar Energy Dept., National Research Centre, Giza, Egypt*

Abstract - *Solar parabolic concentrators are exposed to harsh weather conditions as they are located in open spaces, and therefore the first rows of these solar concentrators are sometimes exposed to strong winds that affect the metal structure of solar concentrators, as well as the accuracy of tracking the concentrates of the sun. The shape of solar concentrates in terms of trough depth, as well as its position while tracking the movement of the sun affects the intensity of the load that the collector itself is exposed to as a result of the wind. this study investigated the effect of the wind on the parabolic trough concentrator in terms of static pressure at parabolic trough depth, rime angle of 90°, 75°, and 60° and at three positions during the tracking movement, the pitch angle of 90°, 45° and 0°. The wind speed contours and the streamlines of the wind flow around the concentrator were presented for all previous cases. The airflow around the parabolic trough concentrator was simulated using the computational fluid dynamics ANSYS -CFD 19.2. From simulation results, it becomes clear that the greater rime angle has a non-significant effect on the pressure resulting from the airflow over the parabolic trough surface. While changing the position of the parabolic trough leads to a significant reduction in the pressure resulted, as the pressure decreases from 264 to 135 Pa, the area where this pressure is affected is also limited.*

Key Words: Parabolic trough concentrator, Wind effect, Solar energy, Static pressure, Simulation.

1. INTRODUCTION

As a result of the successive energy crises in the world for a long time, developed countries began to resort to the use of solar energy and began to manufacture and develop solar concentrates of all kinds to exploit solar thermal energy in generating electricity and in other industrial uses that need medium temperatures. Parabolic trough concentrators (PTC) are one of the best and most widespread types of solar concentrators, due to their high efficiency compared to other types of concentrators. Among the weather factors that directly affect the performance of the parabola concentrators is the speed and direction of the wind on the reflective surface of the solar concentrator. Ruelas et al. studied the effect of wind speed on the design of a solar concentrator, Scheffler type [1]. The performance of the metal structure of the solar concentrator under the influence of winds of up to 180 km/h was investigated using the finite element analysis (FEA) software. The result showed deformations in the steel structure of about 0.005 m and maximum stress of 27 MPa. Peterka et al. investigated in a wind tunnel for a small-scale PTC prototype the effect of the wind on different PTC structures and different focal lengths [2]. They conclude that the gap spacing between collectors in a row did not affect collector loads significantly. Baetzold et al. has carried out researches to reach the optimum shape and layout of parabolic trough concentrators to reduce wind force at the surface of the reflected mirror consequently the steel structure as well as the wind speed around the receiver tube to reduce the thermal losses [3]. They found from the studies that the wind strongly affects the trough of the concentrator at a pitch angle greater than 15 ° and less than -60 °, it also causes large swirls behind the trough surface, which may affect the integrity of the concentrates in the following rows. Sun et al. and others presented a comparison and review of previous research dealing with the force applied by the wind on parabolic concentrates [4].

The parabolic trough collector, which has the same specifications as the LS-2 collector, was developed as the whole metal structure was manufactured from aluminum by Solargenix Company [5]. The tests conducted on the developed PTC in a wind tunnel proved that it meets all requirements in terms of the structure's resistance to bending and torsion. Fu et al. simulate the wind load distribution on the reflecting surface of the PTC with ANSYS software [6]. The computed maximum deflection as a result of taking into account the distribution of the wind load on the trough surface differs by 30% from the calculated maximum deflection based on the average value of the wind load. All previous studies and many other studies focused on investigating the wind effect on only one parabolic trough unit [7-9]. Paetzold et al. studied the effect of the wind load on a field of parabolic trough concentrators consists of several rows behind each other and proved that the collectors on the outer rows are exposed to strong aerodynamic loads depending on the collector shape and the arrangement of the rows [10].

Bootello et al. studied 2D and 3D of the airflow around two types of solar concentrators inside a virtual wind tunnel using a CFD program [11]. The goal was to compare the performance of the two types of PTC one with circular tube and the other with a flat absorber with the parabolic trough type installed in LS-2 and LS-3. Two-dimension numerical simulation of the turbulent flow of wind around the PTC was carried out by Zemler et al. [12]. They get the force and torque values that affect the reflective surface at different pitch angles for parabola width ranges from 1.2 to 3.7 m. A numerical simulation was used to simulate the heat transfer and aerodynamics in detail around a PTC by Hachicha et al. [13]. The model is based on a large vortex around the solar collector. The results showed the presence of many vortices that formed around the reflecting surface and the receiver

tube according to the pitch angle of the solar collector. Zhang et al. made a numerical study to investigate the effect of wind intensity on the optical efficiency of the PTC concerning distortion and the loss in the optical efficiency and also the effect of vibrations resulting from the wind on the optical performance [14]. The study proved that the maximum and minimum deformation of the parabolic trough concentrator occurs at the pitch angle of 0° and 270° respectively. Andre et al. studied the torsional vibration produced by the concentric wind on parabola using large-eddy simulations [15]. The most self-vibrations occurred at the pitch angles that had the largest area of the parabolic mirror are exposed to the vortices, and the large effect of these vortices was found at a pitch angle of 90°. Winkelmann et al. present a wind tunnel test on a parabolic trough concentrator with a large aperture area of 10 m and a module length of 30 m [16]. The experimental and numerical tests included single modules and several modules arranged in rows. The results show that the wind directions of 0°, 30°, 150°, and 180°, as well as the pitch angles of 0°, 45°, and 60°, are the most important that affect the forces on the parabolic trough concentrator.

In this research, studying the effect of air wind flow over the parabolic trough concentrator PTC on the pressure distribution on the surface of the PTC in a virtual wind tunnel was investigated using computational fluid dynamic ANSYS-CFD Software. The performance of a full-scale PTC was performed at different pitch angles. The pressure distribution was investigated at different curve depths though varying the rim angle of the PTC. Also, the airflow streamlines were presented for all previous cases. The rime angle for this study various from 90° to 60° with 15° step. While the pitch angle varied from 90° to 0° with 45° step as shown in Fig. 1.

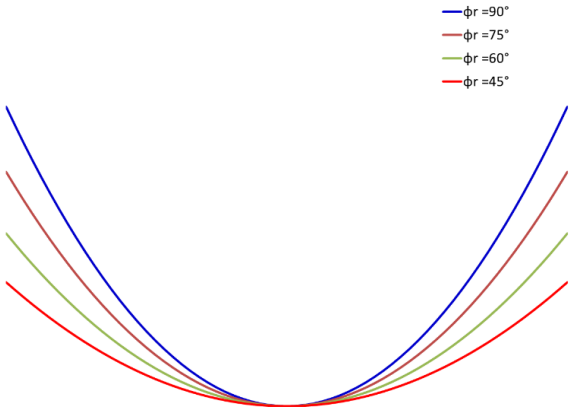

Fig. 1. Different shapes of parabolic trough surface with rime angles ϕ_r of 90°, 75°, 60°, and 45°.

2. Geometry Description

In this study, the flow over the different parabolic shapes with different rime angles was presented. Figure 1 presents a different parabolic trough shape with a rime angle of 90°, 75°, and 60°. The rime angle is defined as the angle between the axis of symmetry and the line that joins the edge of the mirror and the focal point as shown in Fig. 2. The calculations were carried out for three different pitch angle θ which is 90°, 45°, and 0° as shown in Fig. 3.

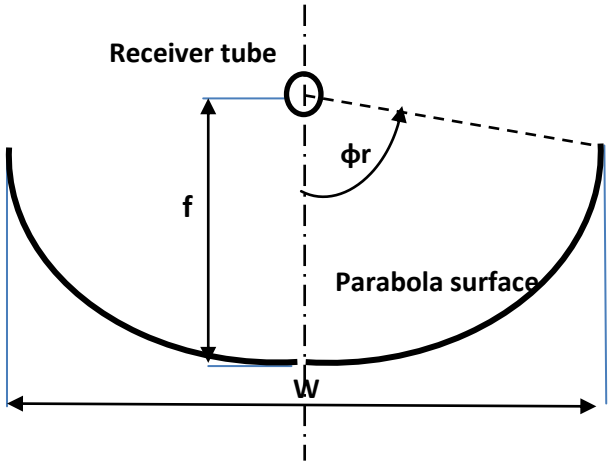

Fig. 2. A Schematic diagram of the parabolic trough concentrator

Fig. 3. Three different pitch angles of the parabolic trough concentrator

The focal length f of the parabolic trough concentrator depends on the parabola width W and the rime angle ϕr as in the following equation:

$$f = \frac{w}{4 * \tan\left(\frac{\phi_r}{2}\right)} \quad [1]$$

The parabolic trough mirror under consideration is 1.6 m in width and 1.9 m in length. The parabolic trough shape depends on the focal length where the Cartesian points pf the parabolic curve can be calculated from the following equation:

$$x^2 = 4 * f * y \quad [2]$$

3. Methodology

The airflow around the parabolic trough concentrator was calculated using the commercial CFD program ANSYS 19.2. at an air wind speed of 15 m/s in the perpendicular direction of the parabola rotation axis. The domain of calculation is

shown in Fig. 4. The origin point is located at the midpoint of the rotation axis of the PTC. The z-axis is directly horizontally normal to the axis of rotation. The x-axis is located horizontally in the same direction as the rotation axis and the y-axis is directly vertical upward. The domine dimension is selected to be 10 m in the stream direction, 3.8 m in the cross direction, and 5.6 m in the perpendicular direction. as shown in Fig. 4. The domine volume was 212.8 m^3. The flow of the air wind velocity was assumed uniform at the inlet of the domine.

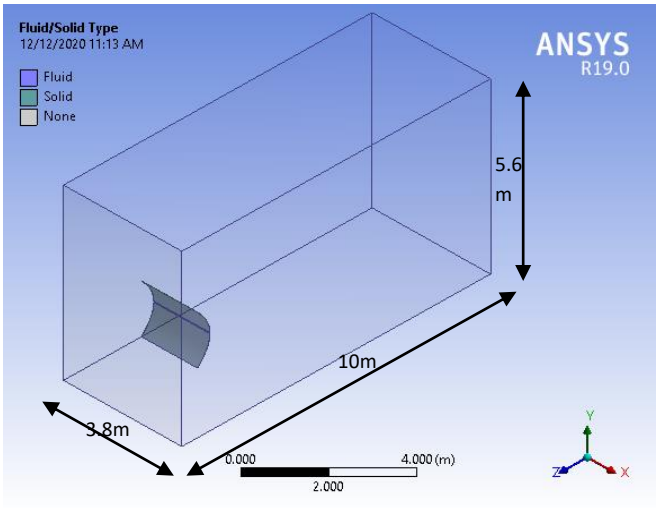

Fig. 4. The domain of the calculation for the parabolic trough mirror at a pitch angle of 90°

The mesh size was chosen so that we obtain an accurate solution to the airflow around the parabolic trough concentrator. The mesh shape and size were refined around the mirror and stretched going away from the mirror as shown in Fig. 5 a) and b). Table 1 presents the statistics and the main characteristics of the mesh model. The wind speed was assumed uniform along with the high of the domain. The numerical simulation was performed under steady-state conditions. The continuity and momentum equations were involved in the simulation. The k-ω turbulence model was used in this simulation. This model is used as an approximation for the Reynolds-averaged Navier–Stokes equations. The model attempts to predict turbulence by two partial differential equations for two variables, k, and ω, with the first variable being the turbulence kinetic energy (k) while the second variable (ω) is the specific rate of heat dissipation.

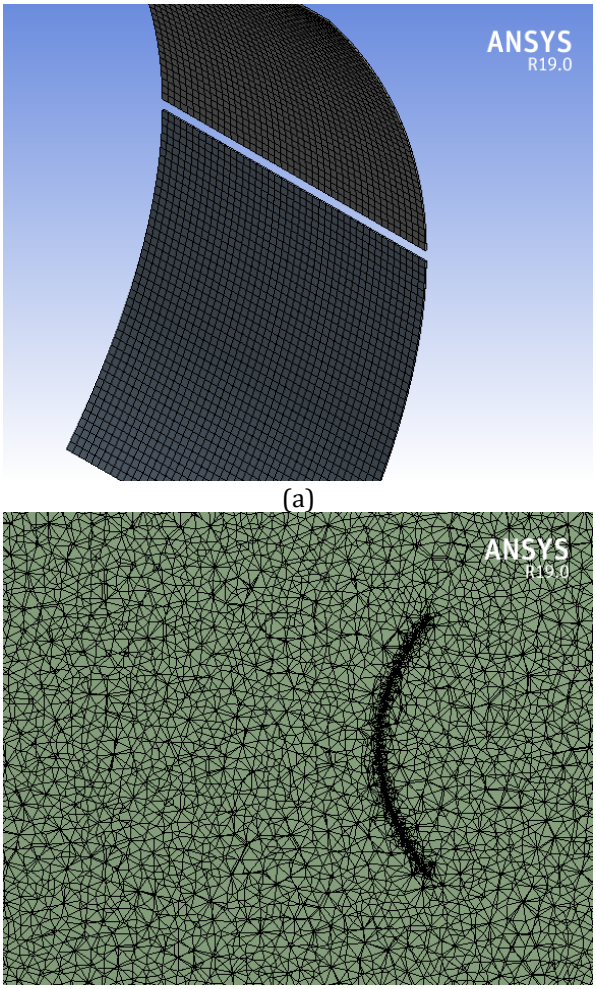

Fig. 5. Mesh distribution for a) the PTC b) around the PTC.

Table 1: Statistics of the mesh model

Item	Value
Mesh	Triangular surface masher
nodes	324832
Elements	1809538
Element size	0.1 m
Geometry	2 body

4. Results and Discussions

The velocity and the steam line of the wind around the parabolic trough concentrator are illustrated in Fig. 6 a), b) and c) for concentrator of rime angle 90° degree and oriented pitch angle θ of 0°, 45°, and 90°, respectively. The calculation was carried at an inlet air velocity of 15 m/s. From the figure, it can be observed that for a pitch angle of 0° there are two big vortexes behind the backside of the parabolic surface. With increasing the oriented pitch angle to 45° a single vortex was formed in the upper part of the

backside of the unnoticeable vortex was formed in the lower part as shown in the figure. At an oriented pitch angle of 90°, it was noticed that no vortex formed around the center of the parabola, but a slight change in the shape of the speed lines was observed, and the speed decreased immediately after the parabolic trough surface.

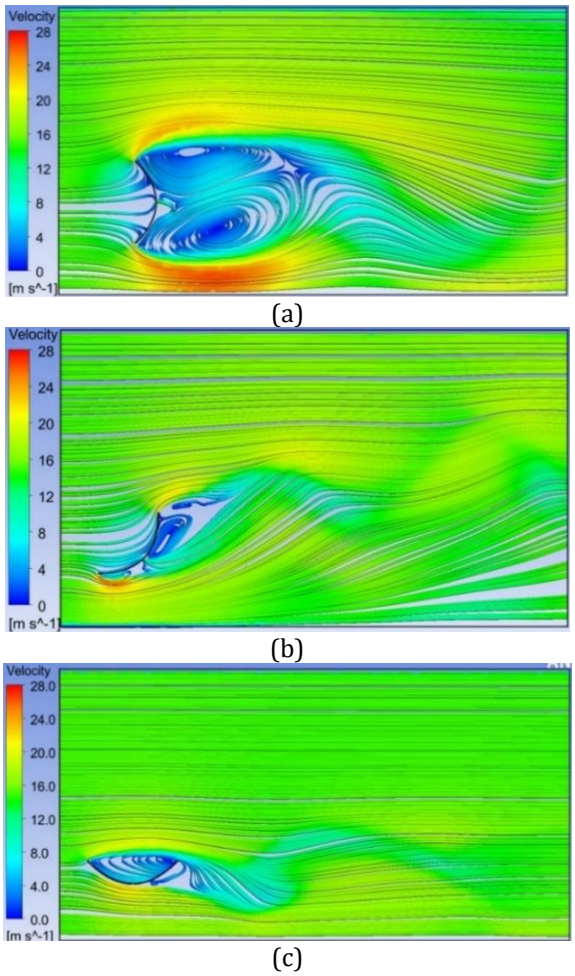

Fig. 6. Velocity steam lines for PTC with 90 rim angle and a pitch angle of a) 90° b) 45° and c) 0°

Figures 7 a), b) and c) show the streamlines of the air velocity for parabolic trough concentrator at rime angle of 75° and a pitch angle of 0°, 45°, and 90°, respectively. It can be noticed that a bigger vortexes diameter at the pitch angle of 0° also at rime angle of 45°, double vortexes were formed in the backside of the parabolic surface also a third small vortex was formed far from the parabolic surface. Figures 8 present the streamline of airflow around the parabolic trough concentrator at a rime angle of 60°. It can be observed low air vortex diameter behind the back surface of the parabolic trough mirror. From figure 6 to 8. It can be concluded that the vortex formed behind the parabolic trough surface has a high diameter in the case of the pitch angle of 0° and rime angle of 75° and 60°.

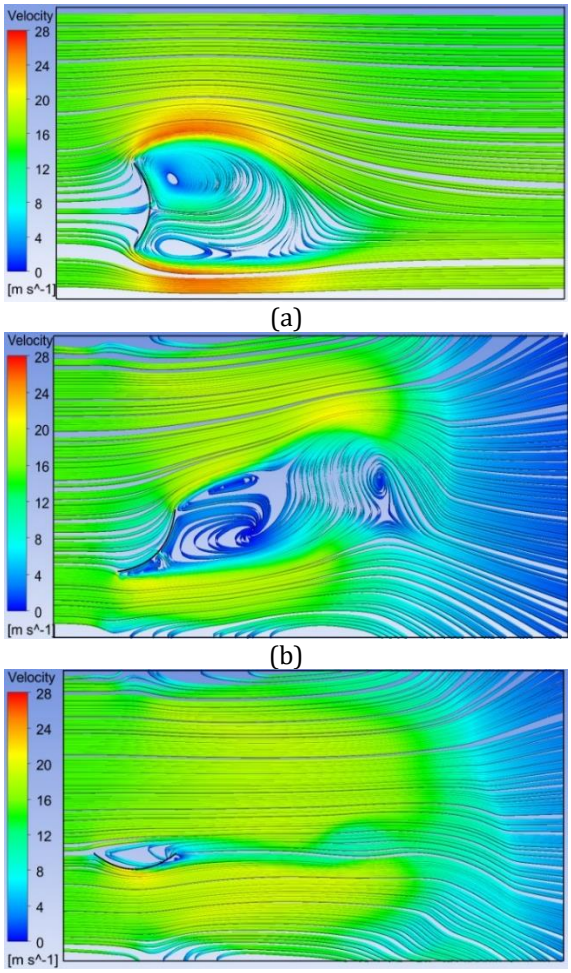

Fig. 7. Velocity steam lines for PTC with 75° rim angle and a pitch angle of a) 90° b) 45° and c) 0°

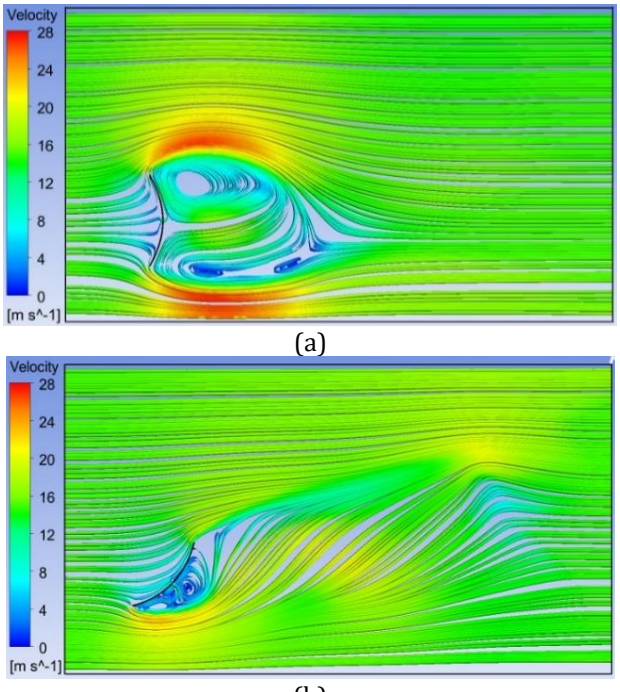

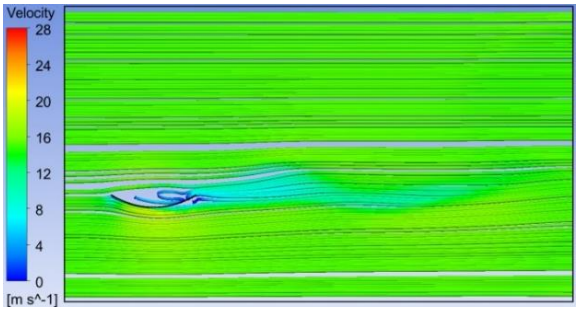

(c)

Fig. 8. Velocity steam lines for PTC with rim angle of 60° and pitch angles of a) 90° b) 45° and)0°.

The velocity pattern of air around the parabolic trough concentrator surface was depicted for three-pitch angles of 0°, 45°, and 90° as shown in Fig. 9 for a rime angle of 90°. It was observed that there were a large air dispersion and a decrease in the air velocity behind the back surface of the parabolic trough concentrator in case of the pitch angle of 0° compared to the case of pitch angle 45° and 90°. The previous observation causes a large drag force affecting the surface of the parabola. In the case of pitch angle 45°, it was observed that the decrease in the air velocity behind the surface of the parabola surface existed in the upper part, and the reign of decreasing the air velocity increases in an upward direction, but their values are much lower than the previous case, the pitch angle of 0°, and this causes a smaller drag force in the upper backside of the parabola surface. The same observation was observed for pitch angle of 90°, but with low values and in a small area that results in low drag force compared to the two previous cases.

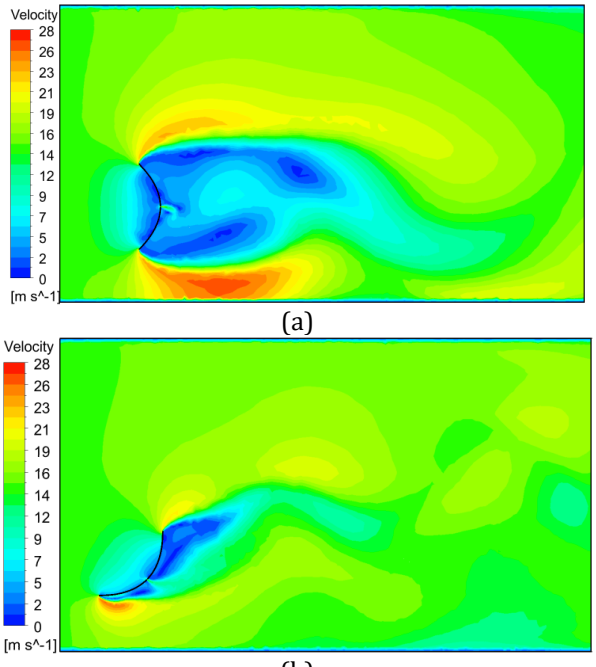

(a)

(b)

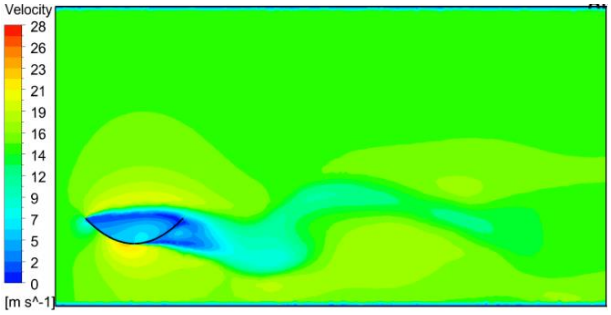

(c)

Fig. 9. Velocity contours diagram for PTC for rime angle of 90° pitch angles of a) 90 b) 45 c) 0

For a rime angle of 75°, the air dispersion is large in the case of a pitch angle of 45° compared to pitch angles of 0° and 90° as shown in Fig. 10. While for rime angles of 60° the air dispersion in the backside of the parabolic surface is lower as shown in Fig. 11. This observation leads to high turbulence and vibration in both sides of the parabolic surface in the case of a rime angle of 75° and a pitch angle of 45° while at a pitch angle of 0 °the air dispersion takes place only on the concave surface for small volume.

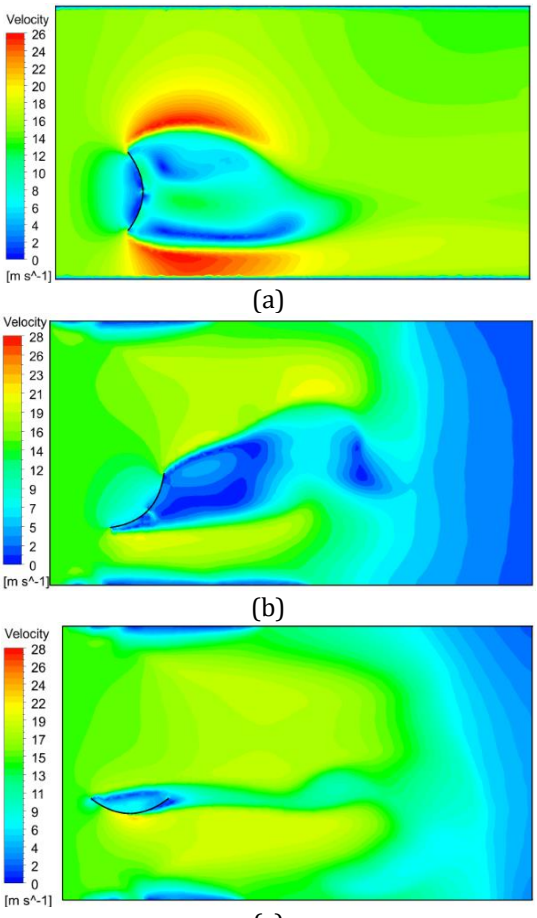

(a)

(b)

(c)

Fig. 10. Velocity contours diagram for PTC at rime angle of 75° and a pitch angle of a) 90° b) 45° c) 0°.

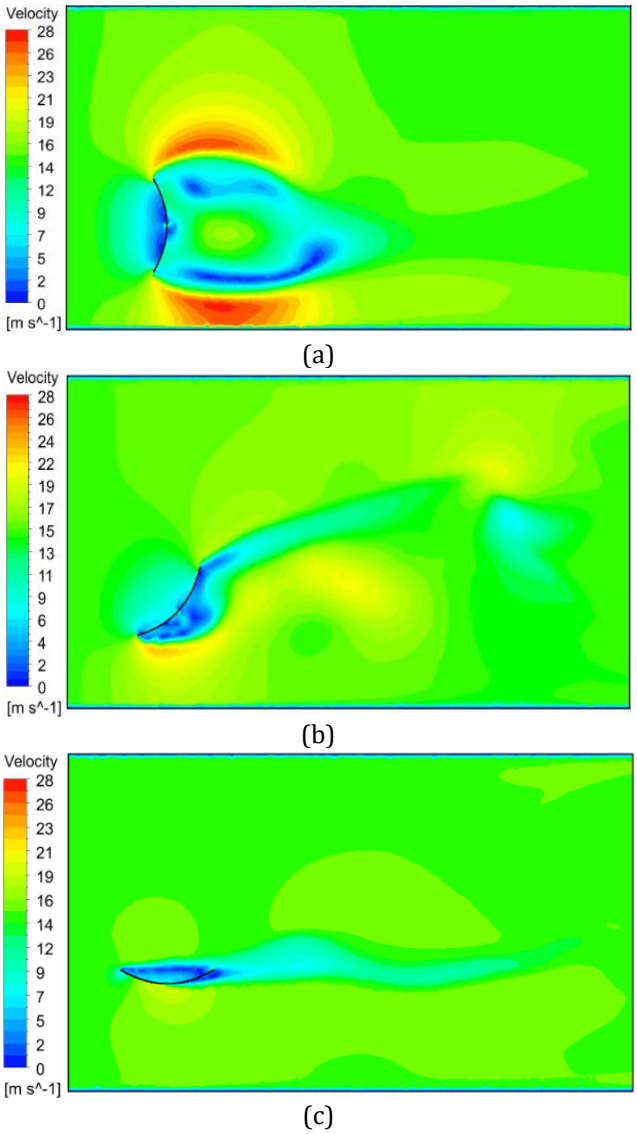

Fig. 11. Velocity contours diagram for PTC at rime angle of 60° and a pitch angle of a) 90° b) 45° c) 0°.

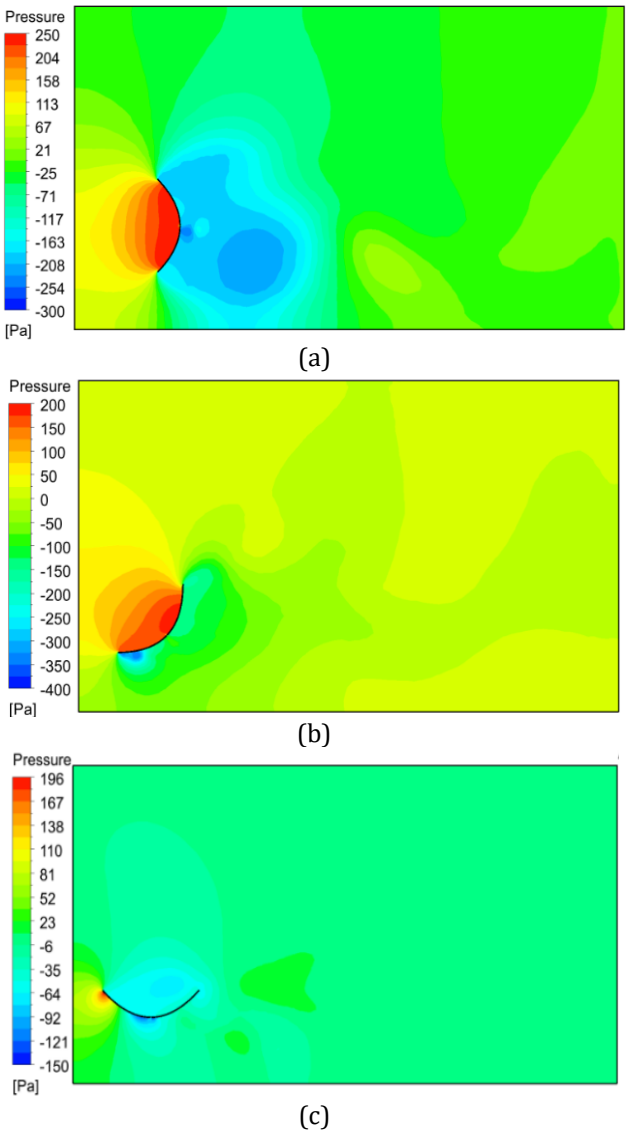

Fig. 12. Pressure contours diagram for PTC at rime angle of 90 ° and a pitch angle of a) 90° b) 45° c) 0°

The pressure contours around the parabolic trough mirrors were presented for parabola rime angles of 90°, 75°, 60°, and 45° in Figs. 12, 13, and 14 respectively. For rime angle of 90°, the pressure contours were presented for pitch angle of 90°, 45°, and 0° as shown in Fig. 12. For a pitch angle of 90°, the pressure contour near the PTC surface is high to about 250 Pa, with a negative pressure reach -300 Pa in a big area behind the parabola surface that means the back surface is subjected to suction force. this value is reduced in the case of a pitch angle of 45° where the front surface is subjected to a pressure of around 200 Pa negative pressure of about -400 Pa but the effect in a very small area of the back surface and the bottom side while for pitch angle of 0° the positive pressure effect in a small part of the parabolic surface by a value not exceed 196 Pa and the top surface is subjected to a negative pressure of -64 Pa and the bottom surface is subjected to little higher value of negative pressure reach –130 Pa.

Figure 13 a), b) and c) present the pressure counter for the parabolic trough mirror at a rime angle of 75° and a pitch angle of 90°, 45°, and 0° respectively. For pitch angle of 90°, it can observe a higher negative value of the pressure behind the back surface compared to the case of rime angle of 90° where the negative value reaches -350 Pa as shown in Fig 13 a). For a pitch angle of 45, the front surface is subjected to positive pressure of 200 Pa in a small area while the backside faces a negative pressure of -120 Pa in the bottom part of the backside. The front positive pressure that effects the parabola mirror is reduced to about 185 Pa in case of the pitch angle of 0°and affects also in a very small area and the back surface is subjected to a negative pressure of -170 Pa at the gap between the mirror parts as shown in Fig. 13 c).

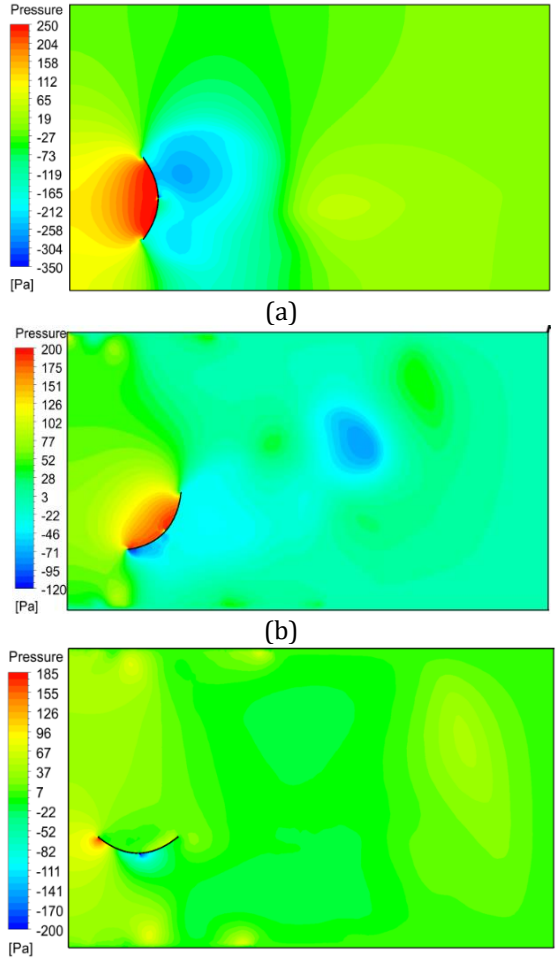

Fig. 13. Pressure contours diagram for PTC at rime angle of 75 ° and a pitch angle of a) 90° b) 45° c) 0°.

Figure 14 a), b) and c) present the pressure counter for the parabolic trough mirror at a rime angle of 60° and a pitch angle of 90°, 45°, and 0° respectively. The positive pressure formed in the front surface was nearly the same for pitch angle of 90° but it was reduced to 165 and 135 Pa for pitch angle of 45° and 0° respectively. The negative pressure affected in the backside of the parabola mirror was reduced to -150 Pa for the pitch angle of 0 only. From the previous observations, it can be concluded that the negative pressure formed behind the back surface can be attributed to the gap between the mirror parts.

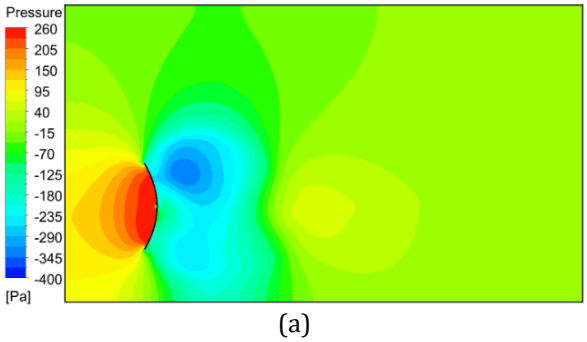

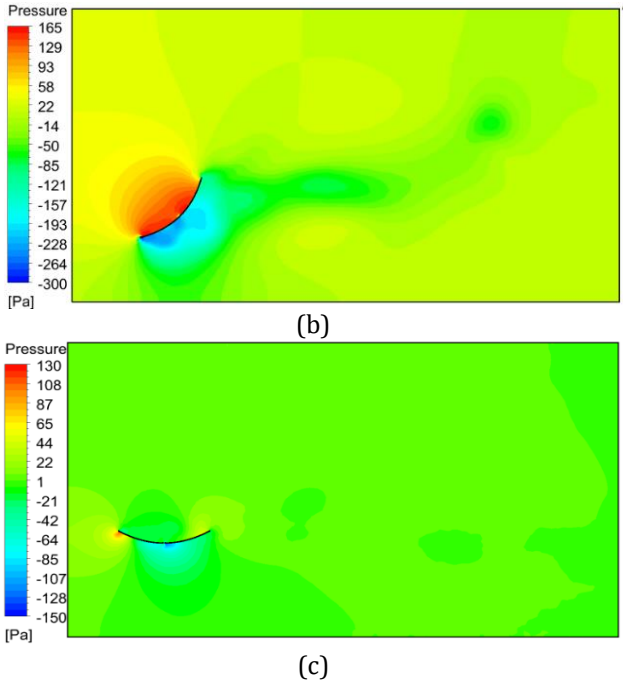

Fig. 14. Pressure contours diagram for PTC at rime angle of 60 ° and a pitch angle of a) 90° b) 45° c) 0°.

5. Conclusion

In this theoretical work, the computational fluid dynamic ANSYS-CFD was used to simulated the air wind over a parabolic trough concentrator at different concentrator rime angles and three-pitch angles. The following conclusions were drawn:

- Studying the different orientations of the PTC by decreasing the pitch angle from 90° to 0°. The results indicated a decrease in the static pressure generated on the front surface of the parabolic trough concentrator where it decreases from 264 to 135 pa respectively.
- Decreasing the rime angle of the parabolic trough concentrator has a non-significant effect on the generated static pressure, where decreasing the rime angle from 90° to 45° has only a change in the generated static pressure by about 7 %.
- It can be also observed large air vortices behind the back surface of the PTC at pitch angles of 90° and 45°, while they decay considerably at a pitch angle of 0° inclination. For a large rime angle, a big diameter of the air vortices was observed.

From the previous conclusions, it is important to point out that the behaviors of the airflow over the parabolic trough concentrator are an important matter to design the supporting steel structure, it also important to design the parabolic shape of the mirror and the safe position through the high wind. Therefore, studying the effect of wind on the strength of the moments that affect PTC at the previous angles is an important topic that needs to be studied in the future.

ACKNOWLEDGEMENT

The author would like to thank the support provided for this work from the Academy of Scientific Research and Technology (ASRT) through the alliance of new and renewable energy (RE _ Alliance)- Made in Egypt project. The author would like also to thank Dr. Radwan Hassan the project coordinator for his support.

REFERENCES

[1] J. Ruelas, A. Cota, F. Ochoa, B. Lucero, T. Burgos, J. Delfin, A. Soto, J. Tzab, J. Lopez & J. Nañez, "Structural Design Methodology for Solar Concentrators Subjected to Wind Loads," Energy Procedia, Vol. 57, 2014, pp. 2872-2878, https://doi.org/10.1016/ j.egypro.2014.10.321.

[2] J. Peterka, J. Sinou, & J. Cermak, "Mean Wind Forces on Parabolic-Trough Solar Collector," Technical Report, Sandia Laboratories, Albuquerque, New Mexico, USA, 1980.

[3] J. Paetzold, S. Cochard, A. Vassallo, & D.F. Fletcher, "Wind engineering analysis of parabolic trough solar collectors: The effects of varying the trough depth," Journal of Wind Engineering and Industrial Aerodynamics, Vol. 135, 2014, pp. 118-128, https://doi.org/10.1016/j.jweia. 2014.10.017.

[4] H. Sun, B. Gong, & Q. Yao, "A review of wind loads on heliostats and trough collectors," Renewable Sustainable Energy Reviews, Vol. 32, 2014, pp. 206–221, https://doi.org/10.1016/j.rser.2014.01.032.

[5] Solar D. (2000). Task 2 Report: New Space-Frame Parabolic Trough Structure. Raleigh, North Carolina: Prepared for NREL by Duke Solar,2000.

[6] W. Fu, M.C. Yang, Y.Z. Zhu & L. Yang, "The wind-structure interaction analysis and optimization of parabolic trough collector," Energy Procedia, Vol. 69, 2015, pp. 77 – 83, https://doi.org/10.1016/j.egypro.2015.03.010.

[7] A.A. Hachicha, I. Rodrı´guez, J. Castro, & A. Oliva, "Numerical simulation of wind flow around a parabolic trough solar collector," Applied Energy, Vol. 107, 2013, pp. 426–437, https://doi.org/10.1016/j.apenergy.2013. 02.014.

[8] N. Hosoya, J. Peterka, R.C. Gee, & D.W Kearney, "Wind tunnel tests of parabolic trough solar collectors wind tunnel tests of parabolic trough solar collectors," Tech. Report, National Renewable Energy Laboratory, Golden, Colorado, USA, 2008.

[9] N. Naeeni, & M. Yaghoubi, "Analysis of wind flow around a parabolic collector (1) fluid flow," Renewable Energy, Vol. 32(11), 2007, pp. 1898–1916, https://doi.org/ 10.1016/j.renene.2006.10.004.

[10] J. Paetzold, S. Cochard, D.F. Fletcher, & A. Vassallo, "Wind Effects in Solar Fields with Various Collector Designs," AIP Conference Proceedings, 1734, 020018, 2016.

[11] J. Bootellom, M. Torrecilla, M. Doblaré, & M. Pérez, "Aerodynamics of new solar parametric troughs: Two dimensional and three dimensional single module numerical analysis," Solar Energy, Vol. 135, 2016, pp. 742-749, https://doi.org/10.1016/j.solener.2016.06. 040.

[12] M.K. Zemler, G. Bohl, O. Rios, & S.K.S. Boetcher, "Numerical study of wind forces on parabolic solar collectors," Renewable Energy, Vol. 60, 2013, pp. 498–505.

[13] A.A. Hachicha, I. Rodrı´guez, & A. Oliva, "Wind speed effect on the flow field and heat transfer around a parabolic trough solar collector," Applied Energy, Vol. 130, 2014, pp. 200–211, https://doi.org/10.1016/ j.apenergy .2014.05.037.

[14] Z. Zhang, J. Sun, L. Wang, J.J. Wei, "Multiphysics-coupled study of wind load effects on optical performance of parabolic trough collector," Solar Energy, Vol. 207, 2020, pp. 1078-1087, https://doi.org/10.1016/j.solener. 2020.06.107D.

[15] M., Andre, M., Péntek, K., Bletzinger, & R. Wüchner, "Aeroelastic simulation of the wind-excited torsional vibration of a parabolic trough solar collector," Journal of Wind Engineering and Industrial Aerodynamics, Vol. 165, 2017, pp. 67-78; https://doi.org/10.1016 /j.jweia.2017.03.005

[16] U. Winkelmann, C. Kamper, R. Hoffer, P. Forman, M.A. Ahrens, & P. Mark, "Wind actions on large-aperture parabolic trough solar collectors: Wind tunnel tests and structural analysis," Renewable Energy, Vol. 146, 2020, pp. 2390- 2407, https://doi.org/10.1016/j.renene. 2019.08.057